Azido inositol probes enable metabolic labeling of inositol-containing glycans and reveal an inositol importer in mycobacteria

Heather Hodges,[1] Kwaku Obeng,[2] Charlotte Avanzi,[1] Alex P. Ausmus,[2] Shiva Kumar Angala,[1] Karishma Kalera,[2,3] Zuzana Palcekova,[1] Benjamin M. Swarts,[2,3]* and Mary Jackson[1]*

[1]Mycobacteria Research Laboratories, Department of Microbiology, Immunology and Pathology, Colorado State University, Fort Collins, CO, 80523 USA

[2]Department of Chemistry and Biochemistry, Central Michigan University, Mount Pleasant, MI, 48859 USA

[3]Biochemistry, Cellular, and Molecular Biology Program, Central Michigan University, Mount Pleasant, MI, 48859 USA

*Corresponding author: E-mail: Mary.Jackson@ColoState.edu

*Corresponding author: E-mail: ben.swarts@cmich.edu

Abstract

Bacteria from the genus *Mycobacterium* include pathogens that cause serious diseases in humans and remain difficult infectious agents to treat. Central to these challenges is the composition and organization of the mycobacterial cell envelope, which includes unique and complex glycans. Inositol is an essential metabolite for mycobacteria due to its presence in the structural core of the immunomodulatory cell envelope glycolipids phosphatidylinositol mannoside (PIM) and PIM-anchored lipomannan (LM) and lipoarabinomannan (LAM). Despite their importance to mycobacterial physiology and pathogenesis, many aspects of PIM, LM, and LAM construction and dynamics remain poorly understood. Recently, probes that allow metabolic labeling and detection of specific mycobacterial glycans have been developed to investigate cell envelope assembly and dynamics. However, these tools have been limited to structures in the mycobacterial cell wall core, including peptidoglycan, arabinogalactan, and mycolic acid-containing glycolipids. Herein, we report the development of synthetic azido inositol (InoAz) analogues as probes that can metabolically label PIMs, LM, and LAM in intact mycobacteria. Additionally, we leverage an InoAz probe to discover an inositol importer and catabolic pathway in *Mycobacterium smegmatis*. We anticipate that in the future, InoAz probes, in combination with bioorthogonal chemistry, will provide a valuable tool for investigating PIM, LM, and LAM biosynthesis, transport, and dynamics in diverse mycobacterial organisms.

Introduction

Mycobacterial species remain a threat to human health and represent some of the most notorious human pathogens, including *Mycobacterium tuberculosis*, *Mycobacterium leprae*, *Mycobacterium ulcerans*, and a number of fast- and slow-growing non-tuberculous mycobacteria. Mycobacteria are collectively characterized by a glycan- and lipid-rich cell envelope that provides antibiotic tolerance and facilitates modulation of the host immune response.[1, 2] Concomitantly, the unique composition and structure of the cell envelope of mycobacterial species is also a diagnostic marker and linchpin therapeutic target.[3, 4] The distinctiveness of these biomolecules among bacteria and their distribution within the mycobacterial cell envelope are suggestive of highly specialized biosynthetic and transport machinery. Interrogation of cell envelope construction and dynamics and, specifically, elucidation of glycan biosynthetic and transport pathways are broadly important to understand the pathology of these microbes and to design therapeutic agents against them.

An important class of glycolipids in the mycobacterial cell envelope are phosphatidylinositol mannosides (PIMs) and their downstream products, lipomannan (LM) and lipoarabinomannan (LAM). PIMs, LM, and LAM are the subject of frequent studies due to their complex structures and critical roles in cellular integrity, permeability, and immunomodulation.[1, 5-7] However, many proteins responsible for PIM/LM/LAM biosynthesis and transport are not known, nor is there knowledge of their dynamics in the cell envelope. The current summary of initial PIM biosynthesis involves the conjugation of one to six mannoses to a phosphatidylinositol (PI) core (**Figure 1**).[1, 8] First, in the cytoplasm, PI is generated by the conjugation of D-*myo*-inositol-3-phosphate to cytidine diphosphate diacylglycerol (CDP-DAG) by the PI synthase PgsA1, followed by a dephosphorylation step catalyzed by an as yet unidentified phosphatase. PI is then mannosylated by GDP-mannose-dependent mannosyltransferases PimA and PimB' at the C2 and C6 positions of inositol, respectively, to generate PIM_1 and PIM_2. Acylation of the C6 hydroxyl of the α-1,2-linked mannose of PIM_1 or PIM_2 is catalyzed by the cytoplasmic acyltransferase, PatA, to produce Ac_1PIM_1 and Ac_1PIM_2. From Ac_1PIM_2 onwards, the mannosyltransferase steps involved in the biosynthesis of Ac_1PIM_6 and LM/LAM are poorly defined. Although PimE has been demonstrated to transform Ac_1PIM_4 to Ac_1PIM_5 on the periplasmic face of the plasma membrane (PM), the protein(s)

responsible for mannosylation of PIM_2 to PIM_4 and PIM_5 to PIM_6 remain to be identified. In addition, which form of PIM is translocated across the PM, and the protein responsible for this key transport step, are still unknown. Elongation of intermediate PIMs to higher PIMs, LM, and LAM on the periplasmic side of the PM involves glycosyltransferases that use the lipid-linked sugar donors decaprenylphospho-mannose (DPM) and decaprenylphospho-arabinose (DPA). In addition to being in the PM, PIM/LM/LAM are also present in the outer mycomembrane (MM), and the LAM-derived polysaccharides D-mannan and arabino-D-mannan have been identified in the capsule of *M. tuberculosis*.[9] However, how these species are transported through the cell envelope to the outer layers is unknown. Additionally, the transporters responsible for the import of PIM/LM/LAM monosaccharide building blocks, including mannose and inositol, have not been previously identified. Finally, there is a lack of information regarding the spatiotemporal dynamics of PIM/LM/LAM construction and turnover during cell growth and division, which significantly lags behind knowledge of dynamics of other cell envelope components, such as peptidoglycan, arabinogalactan, and MM trehalose glycolipids.

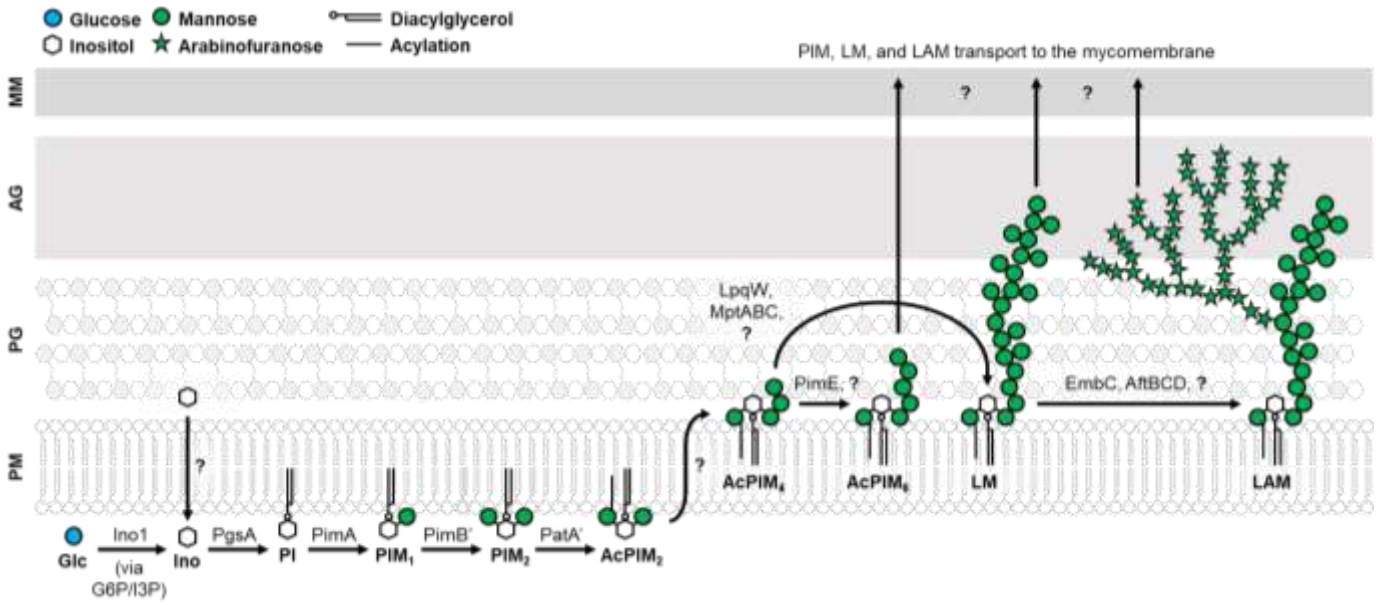

Figure 1. Current knowledge regarding the biosynthesis and transport of PIMs, LM, and LAM. PIM/LM/LAM synthesis is initiated on the cytoplasmic face of the plasma membrane by the addition of two Man*p* residues to phosphatidylinositol (PI) by dedicated, essential, GDP-mannose-dependent mannosyltransferases (PimA and PimB'). Di- or tri-acylated forms of phosphatidylinositol di- or tri-mannosides (PIM_2/Ac_1PIM_2 or PIM_3/Ac_1PIM_3) are then translocated to the periplasmic face of the plasma membrane by (an) as yet unknown inner membrane transporter(s). Elongation of these intermediate PIMs to higher PIMs, LM, and LAM on the periplasmic side of the plasma membrane involves glycosyltransferases (PimE, MptA, MptB, MptC, AftB, AftC, AftD, EmbC) that use lipid-

linked sugar donors (decaprenylphospho-mannose and decaprenylphospho-arabinose). The transporters required to translocate the final PIM, LM and LAM products to the outer leaflet of the outer membrane are not known. See text for further details. AG, arabinogalactan; MM, mycomembrane; PG, peptidoglycan; PM, plasma membrane. Chemical structures of PIMs are shown in Figure 2A.

The above knowledge gaps exist because experimental techniques are limited in their ability to investigate PIM/LM/LAM and their associated biosynthesis and transport pathways. Traditional genetic techniques have uncovered many of the known enzymes in the PIM/LM/LAM pathway. However, mycobacteria are particularly challenging to investigate due to genetic redundancy among transport systems and the use of unique genes to synthesize and transport specialized substrates, limiting the ability to identify these genes from sequence similarity searches.[10] In addition, traditional techniques do not provide a way to track non-genetically encoded glycans and lipids in cellular contexts. A powerful and complementary tool is metabolic labeling with unnatural carbohydrates bearing bioorthogonal handles that can be selectively modified via chemoselective “click” reactions, an approach pioneered by the Bertozzi group.[11] This approach has been applied to develop metabolic labeling tools for various bacterial cell envelope components, which has led to applications in whole-cell imaging, inhibitor development, cell envelope protein discovery, and the creation of novel diagnostic and therapeutic strategies.[12] Synthetic unnatural biosynthetic precursors have been developed to metabolically label an array of mycobacterial cell envelope components, including trehalose- and arabinogalactan-linked mycolates,[13-25] peptidoglycan,[26-28] and arabinogalactan.[29] No such probes have been developed for PIMs or the PIM-anchored derivatives LM and LAM in mycobacteria. The ability to metabolically incorporate inositol-based probes, such as azido inositol (InoAz) analogues, would yield a single substitution in the glycan core of PIMs (or additionally in terminal phospho-inositol capping residues of LAM in relevant organisms) and, in conjunction with bioorthogonal chemistry, would enable researchers to address many of the questions about PIM, LM, and LAM biosynthesis, transport, and dynamics raised above.

Herein, we report the development of InoAz analogues as metabolic labeling probes of PIM, LM, and LAM in the model organism *Mycobacterium smegmatis* (*Msmeg*). We found that 5-position-substituted inositol analogues, including 5-InoAz, are pathway-privileged for incorporation into early PIM species, LM, and LAM, thus providing a new tool to investigate these glycolipids in bacterial cells.

Furthermore, in an effort to improve inositol analogue utilization by *Msmeg* cells, we leveraged 5-InoAz to generate a strain of *Msmeg* harboring mutations in an inositol utilization pathway, which led to the discovery of a previously unknown inositol importer and has implications for enhancing the incorporation of inositol analogues into PIM, LM, and LAM using genetic engineering. Thus, in addition to reporting a new tool for labeling PIM, LM, and LAM, this study highlights the utility of strain evolution approaches toward sugar auxotroph strains to identify spontaneous suppressor mutants that permit or enhance incorporation of azido sugars. Importantly, the ability to metabolically incorporate InoAz probes into PIM, LM, and LAM in live *Msmeg* and perform click chemistry-mediated detection of these species will open the door to addressing key knowledge gaps related to glycolipid biosynthesis and dynamics in mycobacteria.

Results and Discussion

***Design and synthesis of InoAz analogues*.** In considering the possible approaches to developing a metabolic labeling probe for PIM, LM, and LAM, we focused on inositol due to its presence in the structural core of all three glycolipids and the initiating role it plays in their biosynthesis (**Figure 1**). In *Msmeg* and *M. tuberculosis*, it has previously been shown that exogenously supplied inositol can support the growth of inositol auxotrophs lacking *ino1*, suggesting the presence of (a) pathway(s) in these organisms that can potentially be exploited for uptake and metabolic incorporation of InoAz analogues.[30] Because PIM, LM, and LAM are generally unmodified at the 3-, 4-, and 5-positions of the core inositol residue (with the exception of variable acylation at the 3-position), we designed 3-, 4-, and 5-InoAz as probe candidates (**Figures 2A** and **2B**). We anticipated that subtle modification of these positions with small azido groups bearing native stereochemistry might be tolerated by endogenous PIM, LM, and LAM biosynthesis and transport machinery, while the azido group would enable subsequent modification of labeled glycans using azide-specific bioorthogonal chemistries. We envisioned that the InoAz probes would potentially be incorporated into the core of PIM, LM, and LAM, and/or the inositol phosphate cap appended to terminal arabinofuranosyl residues of LAM, a modification that occurs in *Msmeg*.[1] To access the target compounds, we used our recently reported Ferrier carbocyclization-mediated synthesis of

enantiopure InoAz analogues,[31] which was used here to produce 3- and 4-InoAz. Since this method failed to produce 5-InoAz due to an unusual azido group-ejecting elimination side reaction,[31] we used Sureshan's reported regioselective double S_N2 method to generate 5-InoAz.[32]

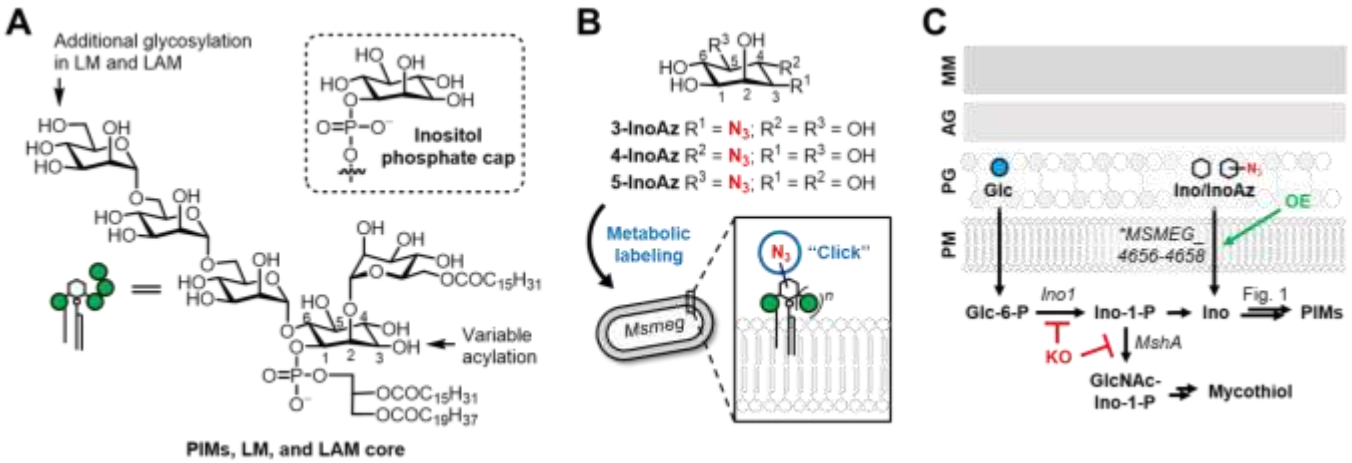

Figure 2. InoAz incorporation into PIM/LM/LAM. (A) Chemical structures of PIMs, LM, LAM. Box, structure of inositol phosphate cap modifying LAM terminal arabinofuranosyl residues in *Msmeg*. (B) Clickable azido inositol (InoAz) analogues and their use as metabolic labeling probes for PIM, LM, and LAM. (C) InoAz incorporation into PIM/LM/LAM and potential knock-out (KO) and overexpression (OE) genetic engineering strategies to favor probe incorporation are shown. *Indicates that this importer was discovered using 5-InoAz in the present work.

***InoAz analogues do not support the growth of an inositol auxotroph*.** As noted above, prior studies revealed the essentiality of inositol and some of its metabolic products, including PI and mono- and dimannosylated forms of PIMs,[33-35] in inositol auxotroph strains of mycobacteria disrupted in *de novo* inositol production, as well as the ability of exogenously supplied inositol to restore activity.[36, 37] Therefore, we reasoned that an *Msmeg* inositol auxotroph (*MsmegΔino1*) would be a good model system to test the ability of our InoAz panel to be incorporated into *Msmeg*, and PIMs in particular, using a simple growth assay. Furthermore, we reasoned that the lack of competition from *de novo*-generated inositol in *MsmegΔino1* would be advantageous for InoAz incorporation (**Figure 2C**). To assess growth rescue, *MsmegΔino1* was grown to saturation with 5 mM inositol, washed to remove residual inositol with inositol-free medium, and then outgrown in inositol-free medium to deplete available inositol in the cytoplasm. Subsequently, the *MsmegΔino1* cells were diluted and supplemented with InoAz analogues and growth was monitored. We observed growth of *MsmegΔino1* in the presence of exogenously supplied inositol

but not in the absence of inositol nor in the presence of 3-, 4-, or 5-InoAz (**Figure S1**). In addition, 3-, 4-, or 5-InoAz up to 10 mM concentration did not inhibit wild-type *Msmeg* growth (data not shown). These results suggested an inability of InoAz analogues to be substituted in place of inositol with high efficiency, due to either a lack of compound import or a downstream bottleneck in the PIM production pathway.

***InoAz analogues differentially label an inositol auxotroph*.** The inability of InoAz analogues to rescue the growth of the *Msmeg*Δ*ino1* strain suggests that the analogues are unable to substitute for native inositol in its metabolic pathways at a level sufficient to support growth. However, the InoAz analogues could be undergoing incorporation into glycolipids at lower levels not sufficient for growth rescue, and/or they may be processed early in the pathway by some enzymes before reaching a bottleneck in incorporation. To investigate these possibilities, we next evaluated the extent of InoAz incorporation into the cell envelope using fluorescent labeling and flow cytometry. Similar to growth assays, wild-type *Msmeg* or inositol auxotroph *Msmeg*Δ*ino1* cells were grown to saturation with 5 mM inositol, then washed into inositol-free medium and starved prior to treatment with InoAz analogues and subsequent labeling with AlexaFluor647 (AF647)-conjugated dibenzocyclooctyne (DBCO-AF647) via a strain-promoted azide−alkyne cycloaddition (SPAAC) reaction. Analysis of fixed cells by flow cytometry revealed that the three InoAz analogues differentially labeled the wild-type and inositol auxotroph strains. 3-InoAz did not measurably incorporate into either strain, whereas 4-InoAz equally labeled both wild-type *Msmeg* and *Msmeg*Δ*ino1* (**Figure S2**). In contrast, whereas 5-InoAz did not incorporate into wild-type *Msmeg*, it efficiently incorporated into the inositol auxotroph *Msmeg*Δ*ino1* when administered at 1 mM concentration (**Figure 3A**). Although the results from 4-InoAz warrant further investigation in the future, the ability of 5-InoAz to efficiently and selectively label *Msmeg*Δ*ino1*, which is indicative of on-target incorporation via inositol metabolism, prompted us to focus on further defining its labeling characteristics in *Msmeg*.

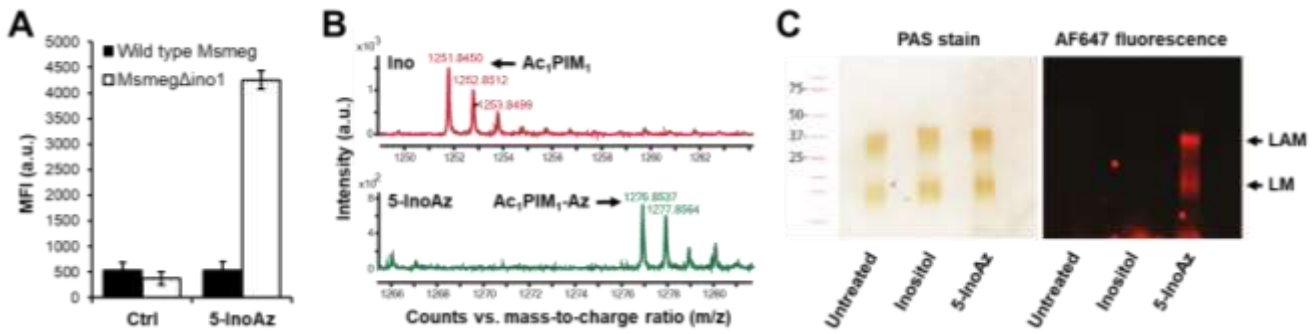

Figure 3. 5-InoAz metabolically labels PIMs, LM, and LAM in an *Msmeg* inositol auxotroph. (A) *Msmeg* wild-type or auxotroph strain *MsmegΔino1* were treated 1 mM inositol (ctrl) or 5-InoAz, reacted with DBCO-AF647 via SPAAC, and analyzed by flow cytometry. Error bars represent the standard deviation of three replicate experiments. See Figure S2 in the Supporting Information for 3- and 4-InoAz labeling results. MFI, Mean Fluorescence Intensity. (B) *MsmegΔino1*,*mshA*::Tn5 was treated with 1 mM inositol or 5-InoAz in 7H9-ADC-tyloxapol medium at 37°C for 12 to 16 hours, then PI and PIMs were extracted and directly analyzed by LC-MS. Data shown are for Ac_1PIM_1 (Ac_1PIM_1 exact mass = 1251.85; Ac_1PIM_1-Az exact mass = 1276.86). See Figure S3 and Table S1 in the Supporting Information for complete LC-MS results. (C) *MsmegΔino1*,*mshA*::Tn5 was untreated (lane 1) or treated with 1 mM inositol (lane 2) or 5-InoAz (lane 3) as described in (B), then LM and LAM were extracted and analyzed by SDS-PAGE using either periodic acid–Schiff silver stain (PAS) (left) or reaction with DBCO-AF647 via SPAAC and fluorescence scanning (right).

5-InoAz incorporates into inositol-containing glycolipids of mycobacteria. To directly examine 5-InoAz incorporation into PI and PIMs, 5-InoAz-treated *Msmeg* samples were subjected to glycolipid isolation and analysis by LC-MS. Note that these experiments were done in a strain we constructed to further favor InoAz incorporation, *MsmegΔino1*,*mshA*::Tn5, which is an inositol auxotroph and furthermore lacks the ability to channel exogenous inositol into the major intracellular reducing thiol in mycobacteria, mycothiol (**Figure 2C**). Using standard extraction procedures, total lipids (PIs and PIMs) were isolated from *MsmegΔino1*,*mshA*::Tn5 treated with either inositol as a control or 5-InoAz as described above for growth and flow cytometry assays. Extracted lipids were analyzed by LC-MS in negative ion mode for the presence of azide-substituted PI and PIMs. Promisingly, in lipid extracts of cells treated with 5-InoAz, we observed peaks corresponding to azide-substituted PI (PI-Az), PIM_1 (PIM_1-Az), and Ac_1PIM_1 (Ac_1PIM_1-Az), directly confirming incorporation of this probe into early PIM species (**Figures 3B** and **S3**, Supporting Information). However, 5-InoAz labeling was not detected in PIM_2, Ac_1PIM_2, or higher PIMs with additional mannosylation, suggesting either inefficient or no labeling of these species (**Figure S3**, Supporting Information), which is consistent with the inability of 5-InoAz to rescue growth of *MsmegΔino1* (**Figure S1**). LC-MS analysis also revealed altered distribution of PIMs in

5-InoAz-treated versus inositol-treated cells, including accumulation of PIM_1 forms and absence of PIM_2 forms (**Table S1**), suggesting a possible bottleneck in the generation of PIM_2 species by the PimB' mannosyltransferase (MSMEG_4253) (see **Figure 1**). In PIM species, the inositol residue is modified at the 1- (phosphoester), 2- (mannose), and 6- (mannose) positions. It is possible that azido group substitution in place of the hydroxyl group at the inositol 5-position disrupts binding to or processing by the PimB' mannosyltransferase at the C6 hydroxyl, but not by upstream PimA at the C2 position. This finding provides insights for future engineering strategies to promote incorporation of 5-InoAz into higher PIM species, such as overexpression or active site engineering of PimB'.

We next used SDS-PAGE to investigate whether 5-InoAz was incorporated into the highly glycosylated PIM derivatives LM and LAM. By SDS-PAGE, LM and LAM separate into two distinct molecular weight fractions that can be detected by periodic acid–Schiff silver stain (PAS), whereas azide labeling can be detected by click chemistry. *Msmeg*Δ*ino1*,*mshA*::Tn5 was treated with 1 mM inositol or 5-InoAz, or left untreated, then LM and LAM were extracted using a standard procedure and subjected to SPAAC reaction with DBCO-AF647 before separation by SDS-PAGE and visualization by in-gel fluorescence scanning. Fluorescence images were then compared to the same gel after PAS staining. LM and LAM extracted from 5-InoAz-treated cells displayed robust fluorescence corresponding to expected LM and LAM bands, whereas unlabeled controls had no detectable signal (**Figure 3C**). The PAS-stained gel showed that each sample had equivalent amounts of LM and LAM material, confirming that the fluorescence signal was azide-specific. In addition, we confirmed that the signal did not originate from unincorporated InoAz that retained in the gel, as the cycloaddition product of DBCO-AF647 incubated with InoAz monosaccharide did not migrate into the LM or LAM regions and instead migrated at the dye front (data not shown).

Together, our LC-MS and SDS-PAGE data demonstrate that, in addition to labeling PIMs up to Ac_1PIM_1, 5-InoAz incorporates into the PIM-anchored glycolipids LM and LAM. Given the apparent bottleneck of 5-InoAz labeling at Ac_1PIM_1 described above, the observed azide-labeling of LM and LAM could be explained by a low level of core inositol labeling, inositol phosphate cap labeling, or both. To provide insight into this issue, we subjected 5-InoAz-labeled LM and LAM extracts to DBCO-AF647

reaction followed by digestion with *Cellulomonas gelida* endoarabinanase, which cleaves internal glycosidic bonds in the LAM arabinan domain, thereby leading to the loss of inositol phosphate-capped arabinan termini.[38] SDS-PAGE analysis of these samples showed that endoarabinanase digestion led to loss of intact LAM and diminished total in-gel fluorescence intensity by ~60%, which is consistent with appreciable incorporation of 5-InoAz into the inositol phosphate LAM capping groups (**Figure S4**). However, following endoarabinanase treatment, ~50% of the fluorescence was still retained in the LM-like band (i.e., endoarabinanase-digested LAM), which, along with the signal in LM from undigested extracts, is indicative of some core labeling (**Figure S4**). Overall, our data are consistent with a scenario in which 5-InoAz labels PIMs, LM, and LAM in *Msmeg*Δ*ino1*,*mshA*::Tn5, with lower PIMs (up to Ac_1PIM_1) being efficiently labeled in the structural core, higher PIM/LM/LAM species having diminished core labeling due to a bottleneck at PimB' required to make PIM_2/Ac_1PIM_2, and LAM being additionally labeled in its inositol phosphate cap. The absence of detectable 5-InoAz-labeled or -unlabeled PIM_2, Ac_1PIM_2, or higher forms of PIMs in 5-InoAz-treated cells while LM and LAM are produced suggests that when inositol incorporation is limited, *Msmeg* favors the synthesis of mature LM and LAM (elongation products of PIM_2/Ac_1PIM_2) over that of intermediate PIM species.

Isolation and sequencing of spontaneous suppressor mutants that allow growth on 5-InoAz. As a potential strategy to overcome bottlenecks associated with 5-InoAz incorporation, we reasoned that extended growth in the presence of 5-InoAz as a singular source of inositol could generate an evolved strain of *Msmeg* able to utilize 5-InoAz more efficiently. As we and others have observed, the metabolic products of native inositol, including PIMs, are required for mycobacterial growth. Therefore, *Msmeg*Δ*ino1*,*mshA*::Tn5 is under strong selective pressure to incorporate 5-InoAz into PIMs. The inability of 5-InoAz-treated cells to replicate (**Figure S1**) provides a simple assay to select strains that have acquired advantageous mutations for growth. *Msmeg*Δ*ino1*,*mshA*::Tn5 was grown to saturation in inositol-containing medium, and then washed and outgrown in inositol-free medium. Cells were then diluted and subjected to extended growth in 7H9 medium that was either supplemented with 1 mM 5-InoAz as the sole source of inositol, or left untreated. Whereas cells that received no additive continued to decline, the culture supplemented with 5-InoAz increased exponentially after a 2-day outgrowth period,

suggesting an acquired ability to utilize 5-InoAz (**Figure 4A**). After 8 days, the 5-InoAz-treated culture was dilution-plated on solid medium containing 1 mM 5-InoAz. Single colonies of ten selected clones were then directly grown in 7H9 liquid medium containing 1 mM 5-InoAz without the need for native inositol, showing that these strains had evolved (a) mechanism(s) that permitted efficient utilization of 5-InoAz as a surrogate for inositol.

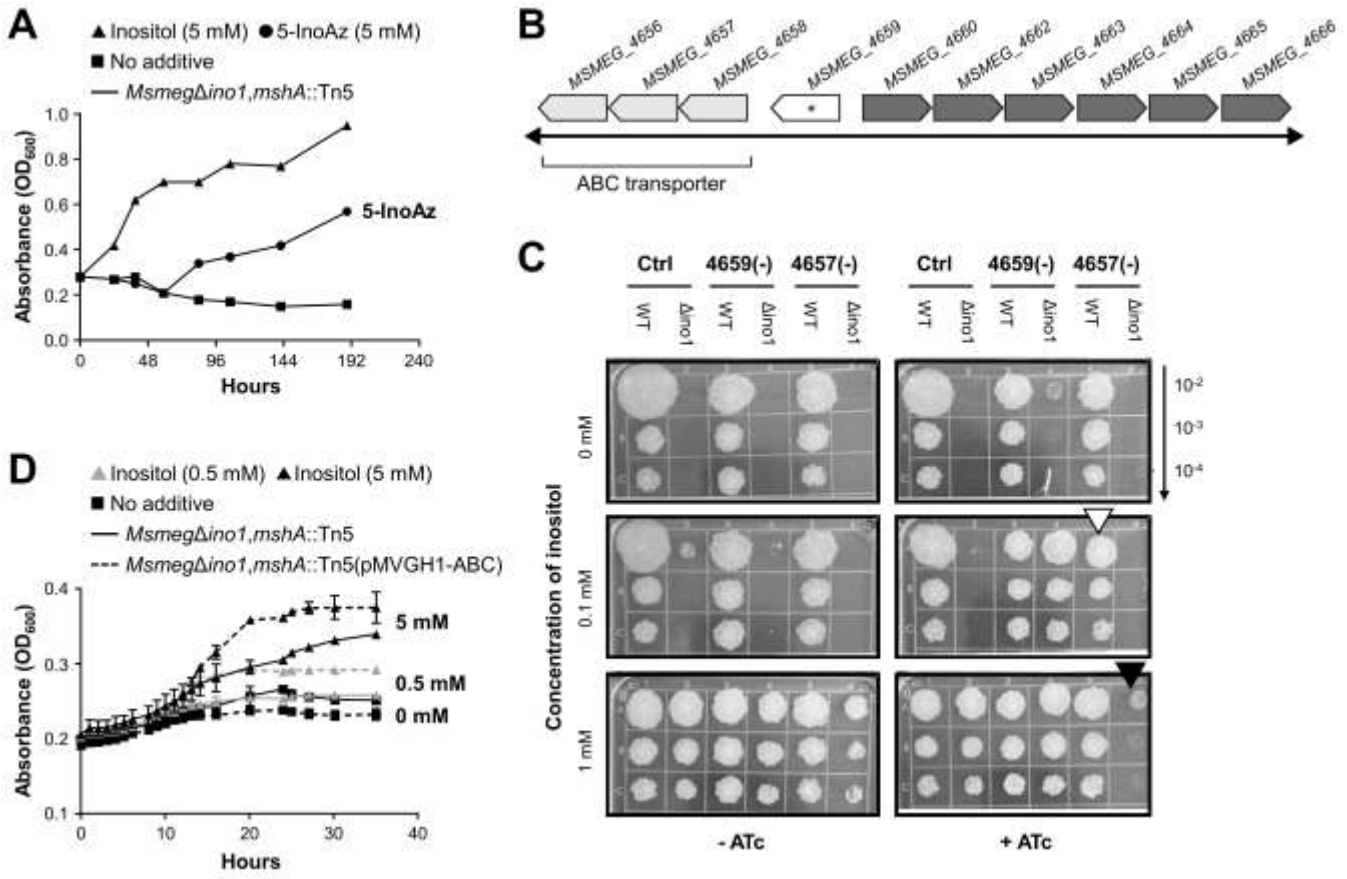

Figure 4. 5-InoAz-derived spontaneous suppressor mutant reveals an inositol utilization pathway in *Msmeg*. (A) *MsmegΔino1*,*mshA*::Tn5 was grown with no additive, 5 mM inositol, or 5 mM 5-InoAz and monitored by optical density at 600 nm over 192 hours. (B) Genetic organization of a potential inositol utilization gene cluster in *Msmeg*. (*) Denotes gene containing mutations observed by whole-genome sequencing. (C) CRISPRi knockdown of *Msmeg* genes of interest, *MSMEG_4657* and *MSMEG_465*9 in wild-type *Msmeg* and *MsmegΔino1*. Strains were transformed with either empty plasmid or plasmid containing a gene-specific guide RNA sequence. Strains were serially diluted on plates without or with ATc (0 or 100 ng/mL) and varied amounts of supplemental inositol (0, 0.1, or 1 mM). Conditional knock-down (cKD) of *MSMEG_4659* supports growth on ten-fold less inositol than parent strain alone and cKD of *MSMEG_4657* abrogates growth of auxotroph. (D) *MsmegΔino1*,*mshA*::Tn5 without and with expression of the ABC transporter MSMEG_4656–4658 was monitored for growth on various amounts of inositol (0, 0.5, and 5 mM) by optical density at 600 nm.

To identify the mutations responsible for permitting growth on 5-InoAz, we performed whole genome sequencing (WGS) of 4 selected suppressor mutant clones from the 5-InoAz-treated culture.

WGS revealed independent non-synonymous mutations in *MSMEG_4659*, which were confirmed by Sanger sequencing in 6 other strains (**Table S2**). All strains harbored frameshift mutations (nucleotide C724insC, C480del, C252insC, C348insA, A270insA) or introduced STOP codons into the *MSMEG_4659* gene sequence (nucleotide C67Y, C235T), with the exception of one isolated clone that harbored a non-synonymous mutation (nucleotide C233T, T>I) in the same gene. All sequenced clones possessed additional mutations in different genes compared to parental control strains, as indicated in **Figure S5**.

Further characterization efforts were focused on the common mutated gene, *MSMEG_4659*. *MSMEG_4659* is predicted to encode a GntR-like bacterial transcription factor (PFAM: PF00392). These transcription factors generally possess an N-terminal DNA-binding domain and a C-terminal oligomerization or effector domain.[39] Furthermore, transcription factors of the GntR family are known to function on carbohydrate metabolism genes.[40] A sequence similarity search to identify the nearest potential homolog of *MSMEG_4659* revealed an intriguing link to a transcription factor IolR, which is involved in the control of inositol catabolism within soil bacteria and *Corynebacterium glutamicum*, a close relative of *Mycobacterium* that possesses PIM, LM, and LAM[41] (IolR, Cgl1057 (cg0196), 55% shared nucleotide identity to *MSMEG_4659*).[42] Our examination of genes immediately downstream of *MSMEG_4659* (**Figure 4B**) revealed a cluster of 6 genes (*MSMEG_4661–MSMEG_4666*) with sequence similarity to genes reported to catabolize inositol to acetyl-CoA and dihydroxyacetone in various soil bacteria.[43] Reports investigating genes under control of IolR in *Corynebacterium glutamicum*[42] also revealed genes involved in inositol importation. Notable in *Msmeg* is the presence of an ABC transporter gene cluster immediately upstream of *MSMEG_4659*, *MSMEG_4656–4658* (**Figure 4B**). The ability of mycobacteria to import inositol has previously been demonstrated from experiments involving inositol auxotrophs[30, 36] and from studies with radiolabeled inositol.[44] Here, we found that wild-type *Msmeg* can grow on inositol (but not 5-InoAz) as a sole carbon source, confirming its ability to import native inositol (**Figure S6**). However, putative transporter genes have only been suggested from bioinformatic analyses for mycobacterial species, and *MSMEG_4656–4658* was not identified as a candidate importer in these studies.[45, 46]

***Silencing* MSMEG_4659 *and* MSMEG_4656–4658 *gene expression reveals roles in inositol utilization*.** To investigate whether the GntR transcriptional repressor MSMEG_4659 and putative ABC-transporter encoded by *MSMEG_4656–4658* played a role in inositol importation or utilization, we used our inositol auxotroph, *Msmeg*Δ*ino1*, to study the effect of silencing these genes on *Msmeg* growth. Since *Msmeg*Δ*ino1* is reliant on the import and utilization of exogenous inositol for growth, silencing genes critical to these functions was expected to lead to the growth arrest of this auxotroph.

We used CRISPR interference (CRISPRi) methodology[47] to knock-down gene expression of *MSMEG_4659* and *MSMEG_*4657, the gene encoding the transmembrane subunit of the adjacent ABC transporter. To silence *MSMEG_4659* and *MSMEG_4657*, plasmids encoding guide RNAs to target these genes were designed according to reported PAM strength guidelines[47] (**Table S3**) and transformed into *Msmeg*Δ*ino1* and wild-type *Msmeg* as a control. *Msmeg*Δ*ino1* strains containing CRISPRi plasmids were maintained in the presence of inositol and no inducer, then washed in inositol-free medium and plated on solid medium with or without inositol (0, 0.1, and 1 mM) and with or without inducer (anhydrotetracycline (ATc); 0 or 100 ng/mL to allow for gene expression or repression, respectively) then incubated alongside wild-type control strains containing CRISPRi plasmids and empty plasmids. As expected, wild-type *Msmeg* grew under all conditions, whereas *Msmeg*Δ*ino1* only grew when supplemented with 1 mM inositol. When *MSMEG_4659* was knocked down in *Msmeg*Δ*ino1* (*MsmegΔino1(MSMEG_4659(-))*), the resulting strain was able to grow on ten-fold less inositol (0.1 mM) (**Figure 4C**), most likely the result of *MSMEG_4659* silencing leading to loss of repression and subsequent enhanced expression of genes involved in inositol importation and/or utilization. In contrast, when *MSMEG_4657*, the gene encoding the transmembrane protein of the *MSMEG_4656–4658* ABC transporter, was silenced in *Msmeg*Δ*ino1* (*MsmegΔino1(MSMEG_4657(-))*), there was a lack of growth on 1 mM inositol (**Figure 4C**), likely due to an inability of the strain to import exogenous inositol. We also designed guide RNAs to target transporters suggested by the literature based on their similarity to known inositol importer genes, including *MSMEG_5166*, *MSMEG_0190*, *MSMEG_5161*, *MSMEG_5559*, and *MSMEG_4462*. We found that when silenced, these genes did not prevent growth on 1 mM inositol in the presence of ATc, indicating that these genes are unlikely to be directly responsible for inositol

importation (**Figure S7**).

Finally, to gain better insight into the function of the ABC transporter MSMEG_4656–4658, we overexpressed the three encoding genes from a replicative plasmid under control of the *hsp60* promoter and monitored growth at 600 nm as a function of exogenously supplied inositol concentrations. We found that the inositol auxotroph strain *Msmeg*Δ*ino1*,*mshA*::Tn5 overexpressing the ABC transporter MSMEG_4656–4658 grew more robustly on inositol and exhibited growth at lower concentrations of inositol than the auxotroph alone (**Figures 4C and 4D**). Combined with the CRISPRi silencing experiments, these results strongly support that MSMEG_4656–4658 is the sole transporter responsible for inositol importation in *Msmeg*.

Conclusion

Inositol-containing glycans in mycobacteria, including PIM, LM, and LAM, have drawn significant attention due to their important roles in the physiology and pathogenesis of multiple human pathogens.[45] Yet, many questions remain regarding the PIM/LM/LAM pathway, including the identity of many proteins involved in their biosynthesis and transport, as well as their dynamics in live cells and during infection. Here, we reported the development and characterization of synthetic InoAz analogues, in particular 5-InoAz, as the first tools for metabolic labeling of these glycolipids. Given the availability of various azide-specific bioorthogonal chemistries and associated strategies for the visualization and enrichment of azide-labeled biomolecules and their interactors,[11, 12] we anticipate that InoAz analogues will open myriad new avenues to investigate the as-yet incompletely characterized PIM/LM/LAM pathway.

In the present work, our screen of three regioisomeric InoAz analogues revealed that the azido group position had a critical impact on metabolic incorporation, which is consistent with previous findings on azide-modified substrates for labeling of trehalose mycolates[14] and arabinogalactan.[29] Our current study mainly focused on the 5-InoAz isomer, which incorporated into early PIMs, LM, and LAM in *Msmeg* strains that were rationally engineered to favor probe incorporation. Furthermore, we took an unbiased genetic approach to improving inositol analogue uptake by growing an inositol auxotroph on 5-InoAz over an extended period, which selected for strains with mutations that enhanced utilization of 5-InoAz.

Characterization of these “evolution” strains led to the discovery of a previously unknown ABC-transporter for inositol import in *Msmeg*, MSMEG_4656–4658 which we here propose to rename InoABC, which represents the first inositol importer identified in mycobacteria. This finding has several implications. First, it highlights the ability of azido sugar probes to elucidate biology through spontaneous mutation approaches, as also recently demonstrated by the use of 6-azido trehalose inhibitory activity to identify PPE51 as the protein required for trehalose uptake across the mycomembrane in *M. tuberculosis*.[48] Second, it suggests next steps for further improving InoAz labeling of PIM, LM, and LAM, including generation of “evolution” strains for other InoAz isomers, as well as overexpressing the inositol importer to favor InoAz uptake. Third, it opens up new avenues for research on mycobacterial inositol metabolism, in particular determining the role of inositol import in mycobacterial physiology and, potentially, virulence.

There are a number of other future directions for the development, characterization, and application of metabolic labeling probes for PIM, LM, and LAM. Herein, we reported both rational and unbiased genetic approaches to improving InoAz incorporation into glycolipids. Additional approaches, such as overexpression or active site engineering of bottleneck enzymes (i.e., PimB’), could also be beneficial. On the other hand, the requirement to genetically alter mycobacteria to enable probe usage can be a limitation, especially with respect to extending the tools to other mycobacterial species. In this regard, it was promising to find that 4-InoAz labeled wild-type *Msmeg*, which we are presently investigating in more detail. In addition, other metabolic precursors to PIM/LM/LAM, such as mannose derivatives or, in the case of LAM, arabinose derivatives, could be pursued as complementary probes for these glycolipids. Additional inositol probe improvement may be achieved through the use of alternative labeling handles (e.g., alkynes), inclusion of extended linkers, and/or a probe design that maintains potential H-bonding interactions, as previously used in the labeling of eukaryotic glycosylphosphatidylinositol (GPI) anchors.[49] In this study, we also discussed the potential of InoAz probes to label the inositol core of PIM/LM/LAM, the inositol phosphate cap of LAM, or both. All of these outcomes are useful, as they enable investigation of complementary aspects of PIM/LM/LAM biosynthesis and export. Overall, novel methods to specifically label PIMs and PIM-derived LM and LAM are expected to be a valuable new addition to the expanding toolbox of mycobacterial cell envelope

probes.

Experimental Procedures

***Strains, culture media, and reagents*.** *M. smegmatis* mc^{2}155 (*Msmeg*) was used as the parental strain, and the mutants derived from it were routinely grown in 7H9 broth supplemented with 0.5% (w/v) glycerol and 10% (v/v) albumin–dextrose–catalase (ADC) and 0.05% tyloxapol at 37°C. The same medium with the addition of 1.5% (w/v) agar was used as solid medium. *Escherichia coli* strain DH5α was maintained in LB medium, propagated at 37°C, and used for routine cloning and transformation experiments. For wash steps, 1X phosphate-buffered saline (PBS, Fisher) was used. Antibiotics, when required, were added at the following concentrations: for *E. coli*, streptomycin 50 μg ml^{-1}, kanamycin 50 μg ml^{-1}; for *Msmeg*, streptomycin 20 μg ml^{-1}, kanamycin 20 μg ml^{-1}, hygromycin 50 μg ml^{-1}, *anhydro*-tetracycline (ATc) 100 ng ml^{-1}. For supplementation with inositol, a high millimolar stock (200–250 mM) of inositol (Sigma) or InoAz was prepared in water. DBCO-AF647 (click chemistry tools) was dissolved in DMSO as a 1 mM stock.

***Chemical Synthesis*.** 3- and 4-InoAz were synthesized as reported by Ausmus et al.[31] 5-InoAz was synthesized as reported by Ravi et al.[32] ^{1}H and ^{13}C NMR spectral data for intermediates and products were acquired on either Varian Mercury 300, Varian Inova 500, or Bruker Avance Neo 500 systems, and matched the literature.

Genetic Manipulations. The construction of an *Msmeg* mc^{2}155 strain that is an auxotroph for inositol involved replacement of the corresponding open reading frame (Ino1: *MSMEG_6904*) with a streptomycin resistance cassette from pHP45Ω following standard allelic replacement strategies with pPR27-xylE, a temperature-sensitive replicative plasmid containing the counter selectable marker *sacB*, and colored marker *xylE*.[50, 51] Briefly, ~500 bp upstream and downstream fragments from *MSMEG_6904* were amplified from primers (**Table S3**) and cloned into shuttle vector pMV261 via isothermal annealing cloning, then the entire cloned segment was digested and ligated into pPR27-xylE generating the plasmid pPR27-xylE-Ino1. This construct was then introduced via electroporation into *Msmeg* mc^{2}155, or an

mshA-interrupted *Msmeg* mc^{2}155 strain containing a Tn5 insertion at *MSMEG_0933* reported previously.[52] Transformants were selected on 7H9 ADC agar plates supplemented with streptomycin (50 µg ml−1) at 30°C. Colonies transformed with pPR27-xylE-ino1 were detected by index plating and development with 1% catechol. pPR27-xylE-ino1 colonies were patched onto 7H9 ADC agar plates containing sucrose (10% w/v), streptomycin (50 µg ml^{-1}), and inositol (5 mM), followed by incubation at 42°C. Insertional mutant colonies were screened for loss of pPR27-xylE-ino1 delivery plasmid by selecting colonies that remained white when sprayed with catechol. These candidate deletion colonies were further validated by replica plating on 7H9 ADC agar plates supplemented with appropriate antibiotics and with and without inositol. Both single (*ino1*: Δ*MSMEG_6904*) and double (*ino1* and *mshA*: Δ*MSMEG_0933*-Δ*MSMEG_6904*) mutants were confirmed by PCR using specific primer combinations for *MSMEG_6904* (**Table S3**) and by whole-genome sequencing.

For CRISPRi plasmids preparation, briefly, PAM sequences were chosen according to predicted strength and sequentially searched in the coding sequence of the gene of interest. Subsequently, sgRNA targeting sequences were designed with two unique BsmBI restriction sites and ligated in CRISPRi plasmid pLJR962.[47]

***Metabolic Labeling*.** For metabolic labeling, cells were washed extensively to remove all residual inositol as indicated in the results section and subsequently cultured in 7H9-ADC-tyloxapol (0.05%) medium supplemented with 1 mM of the indicated InoAz analogue and incubated at 37°C for 12–16 h.

***Fluorescent labeling*.** After metabolic labeling, cells were washed at least 3 times in PBS and resuspended at an optical density of 0.2–0.5 in PBS with 20 µM DBCO-AF647 (1:50, from a 1 mM stock in DMSO) for 30 min at room temperature on a tube rotator in the dark. Fluorescently labeled cells were then washed 3 times in PBS to remove residual dye.

***Flow cytometry*.** Following metabolic and fluorescent labeling, cells were harvested and washed with 1x PBS and transferred to 5 mL polystyrene tubes. Flow cytometry was performed on a three-laser Cytek Aurora flow cytometer. Fluorescence data was collected for 50,000 events, and Flow Cytometry Standard (FCS) file data were analyzed using FlowJo software (BD Biosciences). Gates were set first to reduce scatter and then to select singlets. Histogram data were transformed to calculate mean

fluorescence intensity.

PIM, LM and LAM extraction and analysis. Extraction of PIMs, LM and LAM, digestion of LAM with *Cellulomonas gelida* endoarabinanase and analysis on intact and digested glycolipid and lipoglycan products by TLC, SDS-PAGE and LC/MS followed earlier procedures.[53-57] For samples digested by endoarabinanase,[58, 59] dried samples were resuspended in purified endoarabinanase and incubated overnight in a water bath at 37°C. Samples were then dried in a speed-vac and fluorescently labeled and separated on SDS-PAGE as described above.

Whole genome sequencing. Genomic DNA was extracted from mid-logarithmic phase bacteria growing in 7H9 media using Qiagen UCP Pathogen kit (Qiagen). Illumina libraries were prepared from 830–931 ng of mechanically fragmented DNA (300 bp, Covaris M instrument per manufacturer protocol) using the Kapa Hyper prep kit and quantified using the Qubit double-stranded DNA (dsDNA) BR assay kit (Thermo Fisher Scientific). Fragment size was assessed on a fragment analyzer (Advanced Analytical Technologies). Libraries were multiplexed and sequenced as 75-base-long single-end reads on an Illumina NextSeq 500 instrument. Reads were adapted and quality trimmed with Trimmomatic v0.33 with the following threshold: quality threshold of 15 and minimum length before dropping reads of 40. Trimmed reads were then mapped onto the *Msmeg* mc^{2}155 reference genome (RefSeq NC_008596.1) using Bowtie2 v2.2.5. Variant calling was performed using Varscan (min coverage: 5; min reads: 5; average quality: 15; min variant allele frequency: 0.01; min for homoplasy: 0.9). Vcf were merged with bcftools option –merge.

Data availability. The sequencing data described in this publication have been submitted to the NCBI Gene Expression Omnibus (GEO) under BioProject #PRJNA913569.

Supporting Information

Supporting Tables and Figures include a list of strains, plasmids and primers used in the study; information about the ability of the three Ino-Az probes to support the growth of an *Msmeg* inositol auxotroph and their metabolic incorporation by whole *Msmeg* cells, including into PI/PIM/LM/LAM; a detailed list of the mutations identified in *Msmeg*Δ*ino1*,*mshA*::Tn5 mutants capable of growing on 5-InoAz

as the sole source of inositol; and the results of growth assays to probe the involvement of a number of *Msmeg* potential carbohydrate transporters in inositol import.

Acknowledgements

This work was supported by the National Institute of Allergy and Infectious Diseases (NIAID)/National Institutes of Health (NIH) grants AI064798 and AI155674 (M.J.), National Institute of General Medical Sciences (NIGMS)/National Institutes of Health (NIH) grant GM133080 (H.L.H.), NSF CAREER Award 1654408 (B.M.S.), and Camille and Henry Dreyfus Foundation Henry Dreyfus Teacher–Scholar Award TH-17-034 (B.M.S.). The content is solely the responsibility of the authors and does not necessarily represent the official views of the NIH. NMR instrumentation at Central Michigan University was supported by NSF MRI Award 2117338 (B.M.S.).

References

1. Angala, S. K.; Belardinelli, J. M.; Huc-Claustre, E.; Wheat, W. H.; Jackson, M., The cell envelope glycoconjugates of Mycobacterium tuberculosis. *Critical reviews in biochemistry and molecular biology* **2014,** *49* (5), 361-99.
2. Jarlier, V.; Nikaido, H., Mycobacterial cell wall: Structure and role in natural resistance to antibiotics. *FEMS Microbiol. Lett.* **1994,** *123*, 11-18.
3. Jackson, M., The Mycobacterial Cell Envelope-Lipids. *Cold Spring Harbor perspectives in medicine* **2014,** *4*, a021105.
4. Jackson, M.; McNeil, M. R.; Brennan, P. J., Progress in targeting cell envelope biogenesis in Mycobacterium tuberculosis. *Future microbiology* **2013,** *8* (7), 855-75.
5. Torrelles, J. B.; Schlesinger, L. S., Diversity in Mycobacterium tuberculosis mannosylated cell wall determinants impacts adaptation to the host. *Tuberculosis (Edinb)* **2010,** *90* (2), 84-93.
6. Turner, J.; Torrelles, J. B., Mannose-capped lipoarabinomannan in Mycobacterium tuberculosis pathogenesis. *Pathog Dis* **2018,** *76* (4).
7. Vergne, I.; Gilleron, M.; Nigou, J., Manipulation of the endocytic pathway and phagocyte functions by Mycobacterium tuberculosis lipoarabinomannan. *Front Cell Infect Microbiol* **2015,** *4*, 187.
8. Guerin, M. E.; Korduláková, J.; Alzari, P. M.; Brennan, P. J.; Jackson, M., Molecular basis of phosphatidyl-myo-inositol mannoside biosynthesis and regulation in mycobacteria. *The Journal of biological chemistry* **2010,** *285* (44), 33577-33583.
9. Ortalo-Magne, A.; Andersen, A. B.; Daffe, M., The outermost capsular arabinomannans and other mannoconjugates of virulent and avirulent tubercle bacilli. *Microbiology* **1996,** *142 (Pt 4)*, 927-35.
10. Jackson, M.; Stevens, C. M.; Zhang, L.; Zgurskaya, H. I.; Niederweis, M., Transporters Involved in the Biogenesis and Functionalization of the Mycobacterial Cell Envelope. *Chem Rev* **2021,** *121* (9), 5124-5157.
11. Sletten, E. M.; Bertozzi, C. R., Bioorthogonal chemistry: fishing for selectivity in a sea of functionality. *Angewandte Chemie International Edition* **2009,** *48* (38), 6974-6998.
12. Banahene, N.; Kavunja, H. W.; Swarts, B. M., Chemical reporters for bacterial glycans: development and applications. *Chemical Reviews* **2021,** *122* (3), 3336-3413.
13. Backus, K. M.; Boshoff, H. I.; Barry, C. S.; Boutureira, O.; Patel, M. K.; D'Hooge, F.; Lee, S. S.; Via, L. E.; Tahlan, K.; Barry 3rd, C. E.; Davis, B. G., Uptake of unnatural trehalose analogs as a reporter for Mycobacterium tuberculosis. *Nat. Chem. Biol.* **2011,** *7* (4), 228-235.
14. Swarts, B. M.; Holsclaw, C. M.; Jewett, J. C.; Alber, M.; Fox, D. M.; Siegrist, M. S.; Leary, J. A.; Kalscheuer, R.; Bertozzi, C. R., Probing the mycobacterial trehalome with bioorthogonal chemistry. *J. Am. Chem. Soc.* **2012,** *134* (39), 16123-16126.
15. Foley, H. N.; Stewart, J. A.; Kavunja, H. W.; Rundell, S. R.; Swarts, B. M., Bioorthogonal chemical reporters for selective in situ probing of mycomembrane components in mycobacteria. *Angew. Chem. Int. Edit.* **2016,** *55* (6), 2053-2057.
16. Kavunja, H. W.; Piligian, B. F.; Fiolek, T. J.; Foley, H. N.; Nathan, T. O.; Swarts, B. M., A chemical reporter strategy for detecting and identifying O-mycoloylated proteins in Corynebacterium. *Chem. Commun.* **2016,** *52* (95), 13795-13798.
17. Fiolek, T. J.; Banahene, N.; Kavunja, H. W.; Holmes, N. J.; Rylski, A. K.; Pohane, A. A.; Siegrist, M. S.; Swarts, B. M., Engineering the Mycomembrane of Live Mycobacteria with an Expanded Set of Trehalose Monomycolate Analogues. *ChemBioChem* **2019,** *20* (10), 1282-1291.
18. Peña-Zalbidea, S.; Huang, A. Y. T.; Kavunja, H. W.; Salinas, B.; Desco, M.; Drake, C.; Woodruff, P. J.; Vaquero, J. J.; Swarts, B. M., Chemoenzymatic radiosynthesis of 2-deoxy-2-[18F]fluoro-D-trehalose ([18F]-2-FDTre): A PET radioprobe for in vivo tracing of trehalose metabolism. *Carbohydr. Res* **2019,** *472* (October 2018), 16-22.
19. Kavunja, H. W.; Biegas, K. J.; Banahene, N.; Stewart, J. A.; Piligian, B. F.; Groenevelt, J. M.; Sein, C. E.; Morita, Y. S.; Niederweis, M.; Siegrist, M. S.; Swarts, B. M., Photoactivatable Glycolipid Probes for Identifying Mycolate–Protein Interactions in Live Mycobacteria. *J. Am. Chem. Soc.* **2020,** *142* (17), 7725-7731.

20. Rundell, S. R.; Wagar, Z. L.; Meints, L. M.; Olson, C. D.; O'Neill, M. K.; Piligian, B. F.; Poston, A. W.; Hood, R. J.; Woodruff, P. J.; Swarts, B. M., Deoxyfluoro-D-trehalose (FDTre) analogues as potential PET probes for imaging mycobacterial infection. *Org. Biomol. Chem.* **2016,** *14* (36), 8598-8609.
21. Kamariza, M.; Shieh, P.; Ealand, C. S.; Peters, J. S.; Chu, B.; Rodriguez-Rivera, F. P.; Babu Sait, M. R.; Treuren, W. V.; Martinson, N.; Kalscheuer, R.; Kana, B. D.; Bertozzi, C. R., Rapid detection of *Mycobacterium tuberculosis* in sputum with a solvatochromic trehalose probe. *Sci. Transl. Med.* **2018,** *10* (430), eaam6310-eaam6310.
22. Banahene, N.; Swarts, B. M., Metabolic Labeling of Live Mycobacteria with Trehalose-Based Probes. In *Mycobacteria Protocols*, Parish, T.; Kumar, A., Eds. Springer US: New York, NY, 2021; pp 385-398.
23. Biegas, K. J.; Swarts, B. M., Chemical probes for tagging mycobacterial lipids. *Curr. Opin. Chem. Biol.* **2021,** *65*, 57-65.
24. Banahene, N.; Gepford, D. M.; Biegas, K. J.; Swanson, D. H.; Hsu, Y.-P.; Murphy, B. A.; Taylor, Z. E.; Lepori, I.; Siegrist, M. S.; Obregón-Henao, A.; VanNieuwenhze, M. S.; Swarts, B. M., Far-Red Molecular Rotor Fluorogenic Trehalose Probe for Live Mycobacteria Detection and Drug-Susceptibility Testing. *Angew. Chem. Int. Edit.* **2022,** *n/a* (n/a).
25. Pohane, A. A.; Moore, D. J.; Lepori, I.; Gordon, R. A.; Nathan, T. O.; Gepford, D. M.; Kavunja, H. W.; Swarts, B. M.; Siegrist, M. S., A Bifunctional Chemical Reporter for in Situ Analysis of Cell Envelope Glycan Recycling in Mycobacteria. *ACS Infect. Dis.* **2022,** *8* (11), 2223-2231.
26. Kuru, E.; Velocity Hughes, H.; Brown, P. J.; Hall, E.; Tekkam, S.; Cava, F.; de Pedro, M. A.; Brun, Y. V.; VanNieuwenhze, M. S., In situ Probing of Newly Synthesized Peptidoglycan in Live Bacteria with Fluorescent D-Amino Acids. *Angew. Chem. Int. Edit.* **2012,** *51* (50), 12519-12523.
27. Siegrist, M. S.; Whiteside, S.; Jewett, J. C.; Aditham, A.; Cava, F.; Bertozzi, C. R., (D)-Amino acid chemical reporters reveal peptidoglycan dynamics of an intracellular pathogen. *ACS Chem Biol* **2013,** *8* (3), 500-5.
28. Liang, H.; DeMeester, K. E.; Hou, C. W.; Parent, M. A.; Caplan, J. L.; Grimes, C. L., Metabolic labelling of the carbohydrate core in bacterial peptidoglycan and its applications. *Nat. Commun.* **2017,** *8*, 15015.
29. Marando, V. M.; Kim, D. E.; Calabretta, P. J.; Kraft, M. B.; Bryson, B. D.; Kiessling, L. L., Biosynthetic glycan labeling. *Journal of the American Chemical Society* **2021,** *143* (40), 16337-16342.
30. Movahedzadeh, F.; Smith, D. A.; Norman, R. A.; Dinadayala, P.; Murray-Rust, J.; Russell, D. G.; Kendall, S. L.; Rison, S. C.; McAlister, M. S.; Bancroft, G. J., The Mycobacterium tuberculosis ino1 gene is essential for growth and virulence. *Molecular microbiology* **2004,** *51* (4), 1003-1014.
31. Ausmus, A. P.; Hogue, M.; Snyder, J. L.; Rundell, S. R.; Bednarz, K. M.; Banahene, N.; Swarts, B. M., Ferrier carbocyclization-mediated synthesis of enantiopure azido inositol analogues. *The Journal of Organic Chemistry* **2020,** *85* (5), 3182-3191.
32. Ravi, A.; Hassan, S. Z.; Vanikrishna, A. N.; Sureshan, K. M., Regioselective SN 2 reactions for rapid syntheses of azido-inositols by one-pot sequence-specific nucleophilysis. *Chemical Communications* **2017,** *53* (28), 3971-3973.
33. Guerin, M. E.; Kaur, D.; Somashekar, B. S.; Gibbs, S.; Gest, P.; Chatterjee, D.; Brennan, P. J.; Jackson, M., New insights into the early steps of phosphatidylinositol mannoside biosynthesis in mycobacteria: PimB' is an essential enzyme of *Mycobacterium smegmatis*. *The Journal of biological chemistry* **2009,** *284* (38), 25687-25696.
34. Jackson, M.; Crick, D. C.; Brennan, P. J., Phosphatidylinositol is an essential phospholipid of mycobacteria. *The Journal of biological chemistry* **2000,** *275* (39), 30092-30099.
35. Korduláková, J.; Gilleron, M.; Mikušová, K.; Puzo, G.; Brennan, P. J.; Gicquel, B.; Jackson, M., Definition of the first mannosylation step in phosphatidylinositol mannoside synthesis. PimA is essential for growth of mycobacteria. *The Journal of biological chemistry* **2002,** *277* (35), 31335-44.
36. Haites, R. E.; Morita, Y. S.; McConville, M. J.; Billman-Jacobe, H., Function of phosphatidylinositol in mycobacteria. *Journal of Biological Chemistry* **2005,** *280* (12), 10981-10987.
37. Jackson, M.; Crick, D. C.; Brennan, P. J., Phosphatidylinositol is an essential phospholipid of mycobacteria. *Journal of Biological Chemistry* **2000,** *275* (39), 30092-30099.

38. Shi, L.; Berg, S.; Lee, A.; Spencer, J. S.; Zhang, J.; Vissa, V.; McNeil, M. R.; Khoo, K.-H.; Chatterjee, C., The carboxy terminus of EmbC from *Mycobacterium smegmatis* mediates chain length extension of the arabinan in lipoarabinomannan. *J. Biol. Chem* **2006,** *281* (28), 19512-19526.
39. Haydon, D. J.; Guest, J. R., A new family of bacterial regulatory proteins. *FEMS microbiology letters* **1991,** *79* (2-3), 291-296.
40. Li, Z.; Xiang, Z.; Zeng, J.; Li, Y.; Li, J., A GntR family transcription factor in Streptococcus mutans regulates biofilm formation and expression of multiple sugar transporter genes. *Frontiers in microbiology* **2019,** *9*, 3224.
41. Tatituri, R. V. V.; Illarionov, P. A.; Dover, L. G.; Nigou, J.; Gilleron, M.; Hitchen, P.; Krumbach, K.; Morris, H. R.; Spencer, N.; Dell, A.; Eggeling, L.; Besra, G. S., Inactivation of Corynebacterium glutamicum NCgl0452 and the Role of MgtA in the Biosynthesis of a Novel Mannosylated Glycolipid Involved in Lipomannan Biosynthesis**The costs of publication of this article were defrayed in part by the payment of page charges. This article must therefore be hereby marked "advertisement" in accordance with 18 U.S.C. Section 1734 solely to indicate this fact. *J. Biol. Chem.* **2007,** *282* (7), 4561-4572.
42. Klaffl, S.; Brocker, M.; Kalinowski, J.; Eikmanns, B. J.; Bott, M., Complex regulation of the phosphoenolpyruvate carboxykinase gene pck and characterization of its GntR-type regulator IolR as a repressor of myo-inositol utilization genes in Corynebacterium glutamicum. *Journal of bacteriology* **2013,** *195* (18), 4283-4296.
43. Yoshida, K.-i.; Yamaguchi, M.; Morinaga, T.; Kinehara, M.; Ikeuchi, M.; Ashida, H.; Fujita, Y., myo-Inositol catabolism in Bacillus subtilis. *Journal of Biological Chemistry* **2008,** *283* (16), 10415-10424.
44. Newton, G. L.; Ta, P.; Bzymek, K. P.; Fahey, R. C., Biochemistry of the initial steps of mycothiol biosynthesis. *Journal of Biological Chemistry* **2006,** *281* (45), 33910-33920.
45. Reynolds, T. B., Strategies for acquiring the phospholipid metabolite inositol in pathogenic bacteria, fungi and protozoa: making it and taking it. *Microbiology* **2009,** *155* (Pt 5), 1386.
46. Morita, Y. S.; Fukuda, T.; Sena, C. B.; Yamaryo-Botte, Y.; McConville, M. J.; Kinoshita, T., Inositol lipid metabolism in mycobacteria: biosynthesis and regulatory mechanisms. *Biochimica et Biophysica Acta (BBA)-General Subjects* **2011,** *1810* (6), 630-641.
47. Rock, J. M.; Hopkins, F. F.; Chavez, A.; Diallo, M.; Chase, M. R.; Gerrick, E. R.; Pritchard, J. R.; Church, G. M.; Rubin, E. J.; Sassetti, C. M., Programmable transcriptional repression in mycobacteria using an orthogonal CRISPR interference platform. *Nature microbiology* **2017,** *2* (4), 1-9.
48. Sait, M. R. B.; Koliwer-Brandl, H.; Stewart, J. A.; Swarts, B. M.; Jacobsen, M.; Ioerger, T. R.; Kalscheuer, R., PPE51 mediates uptake of trehalose across the mycomembrane of Mycobacterium tuberculosis. *Scientific Reports* **2022,** *12*.
49. Ricks, T. J.; Cassilly, C. D.; Carr, A. J.; Alves, D. S.; Alam, S.; Tscherch, K.; Yokley, T. W.; Workman, C. E.; Morrell-Falvey, J. L.; Barrera, F. N., Labeling of Phosphatidylinositol Lipid Products in Cells through Metabolic Engineering by Using a Clickable myo-Inositol Probe. *ChemBioChem* **2019,** *20* (2), 172-180.
50. Jackson M; Camacho LR; Gicquel B; C.., G.; Parish T; NG, S., *Gene replacement and transposon delivery using the negative selection marker sacB*. Humana Press: 2001; Vol. 54.
51. Pelicic, V.; Reyrat, J. M.; Gicquel, B., Generation of unmarked directed mutations in mycobacteria, using sucrose counter-selectable suicide vectors. *Mol Microbiol* **1996,** *20* (5), 919-25.
52. Newton, G. L.; Koledin, T.; Gorovitz, B.; Rawat, M.; Fahey, R. C.; Av-Gay, Y., The glycosyltransferase gene encoding the enzyme catalyzing the first step of mycothiol biosynthesis (mshA). *Journal of Bacteriology* **2003,** *185* (11), 3476-3479.
53. Kaur, D.; McNeil, M. R.; Khoo, K. H.; Chatterjee, D.; Crick, D. C.; Jackson, M.; Brennan, P. J., New insights into the biosynthesis of mycobacterial lipomannan arising from deletion of a conserved gene. *The Journal of biological chemistry* **2007,** *282* (37), 27133-27140.
54. Palcekova, Z.; Angala, S. K.; Belardinelli, J. M.; Eskandarian, H. A.; Joe, M.; Brunton, R.; Rithner, C.; Jones, V.; Nigou, J.; Lowary, T. L.; Gilleron, M.; McNeil, M.; Jackson, M., Disruption of the SucT acyltransferase in *Mycobacterium smegmatis* abrogates succinylation of cell envelope polysaccharides. *The Journal of biological chemistry* **2019,** *294* (26), 10325-10335.

55. Palcekova, Z.; Gilleron, M.; Angala, S. K.; Belardinelli, J. M.; McNeil, M.; Bermudez, L. E.; Jackson, M., Polysaccharide Succinylation Enhances the Intracellular Survival of Mycobacterium abscessus. *ACS Infect Dis* **2020,** *6* (8), 2235-2248.
56. Sartain, M. J.; Dick, D. L.; Rithner, C. D.; Crick, D. C.; Belisle, J. T., Lipidomic analyses of Mycobacterium tuberculosis based on accurate mass measurements and the novel "Mtb LipidDB"[S]. *Journal of lipid research* **2011,** *52* (5), 861-872.
57. Prinzis, S.; Chatterjee, D.; Brennan, P. J., Structure and antigenicity of lipoarabinomannan from Mycobacterium bovis BCG. *Microbiology* **1993,** *139* (11), 2649-2658.
58. Chatterjee, D.; Khoo, K.-H., Mycobacterial lipoarabinomannan: an extraordinary lipoheteroglycan with profound physiological effects. *Glycobiology* **1998,** *8* (2), 113-120.
59. McNeil, M. R.; Robuck, K. G.; Harter, M.; Brennan, P. J., Enzymatic evidence for the presence of a critical terminal hexa-arabinoside in the cell walls of Mycobacterium tuberculosis. *Glycobiology* **1994,** *4* (2), 165-174.

TOC Graphic

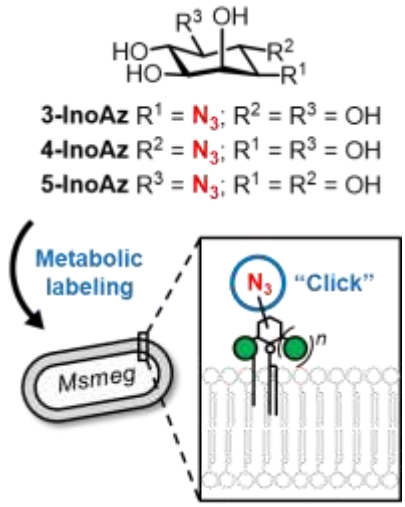
R3 OH
HO
HO
R2
R1
3-InoAz R1 = N3; R2 = R3 = OH
4-InoAz R2 = N3; R1 = R3 = OH
5-InoAz R3 = N3; R1 = R2 = OH
Metabolic labeling
Msmeg
N3
"Click"
n